

# Black Mirrors: CPT-Symmetric Alternatives to Black Holes

Kostas Tzanavaris,<sup>1</sup> Latham Boyle,<sup>1,2</sup> and Neil Turok<sup>1,2</sup>

<sup>1</sup>*Higgs Centre for Theoretical Physics, James Clerk Maxwell Building, Edinburgh EH9 3FD, UK*  
<sup>2</sup>*Perimeter Institute for Theoretical Physics, Waterloo, Ontario N2L 2Y5, Canada*

Einstein’s equations imply that a gravitationally collapsed object forms an event horizon. But what lies on the other side of this horizon? In this paper, we question the reality of the conventional solution (the black hole), and point out another, topologically distinct solution: the *black mirror*. In the black hole solution, the horizon connects the exterior metric to an interior metric which contains a curvature singularity. In the black mirror, the horizon instead connects the exterior metric to its own CPT mirror image, yielding a solution with no curvature singularities. We give the general stationary (charged, rotating) black mirror solution explicitly, and also describe the general black mirror formed by gravitational collapse. The black mirror is the relevant stationary point when the quantum path integral is equipped with suitably CPT-symmetric boundary conditions, that we propose. It appears to avoid many vexing puzzles which plague the conventional black hole.

## I. INTRODUCTION

The Einstein-Rosen bridge (the first wormhole geometry) was put forth by Einstein and Rosen in [1]. One of their motivations was to get rid of the apparent “singularity” at the event horizon  $r = 2m$  by introducing a new coordinate  $u$  by  $r = 2m + u^2$ , and letting  $u$  extend over  $-\infty < u < \infty$ . This describes two Schwarzschild exteriors (regions  $I$  and  $I'$  in Fig. 1a), glued at the radius  $r = 2m$  (the midpoint in Fig. 1a). However, it was later deemed to be unphysical as the papers of Oppenheimer-Snyder [2] describing spherical collapse showed that the singularity at  $r = 2m$  is just a coordinate singularity, and an infalling observer following the collapsing matter will not feel anything unusual happening at the event horizon. This (and other developments) led to the modern belief that the black hole interior really exists, and that the black hole’s horizon is completely non-singular.

Nevertheless, the modern black hole picture of gravitational collapse is not without its problems. Aside from the emergence of curvature singularities, there are other problems that the currently accepted theories cannot address adequately, including the breakdown of causality, *i.e.*, the emergence and stability of Cauchy horizons [3], as well as the information [4] and firewall [5] paradoxes.

In this paper, we argue that certain natural modifications of Einstein-Rosen bridges – which we call *black mirrors* – are, in fact, direct consequences of CPT symmetry, and offer novel solutions to the problems mentioned above, along with other merits discussed below.<sup>1</sup>

## II. THE SCHWARZSCHILD BLACK MIRROR

For simplicity, let us first consider the Schwarzschild metric, describing an eternal, static, uncharged object.

In Schwarzschild coordinates  $(r, t)$  it is

$$ds^2 = -f(r)dt^2 + \frac{dr^2}{f(r)} + r^2d\Omega^2 \quad (1)$$

where

$$f(r) \equiv 1 - \frac{2m}{r} \quad \text{and} \quad d\Omega^2 \equiv d\theta^2 + \sin^2\theta d\varphi^2. \quad (2)$$

This solution has a horizon at  $r = 2m$ , the root of  $f(r)$ . Note that Schwarzschild coordinates only cover the exterior region  $r > 2m$ , and become singular at the horizon  $r = 2m$  (which lies at  $t = \pm\infty$  in these coordinates).

The conventional view is that the *full* spacetime (including the horizon, and what lies behind it) is the maximal analytic extension obtained by switching from Schwarzschild to Kruskal coordinates [12]. The Penrose diagram of this extension is shown in Fig. 1a: it has two exterior regions  $I, I'$ , two interior regions  $II, II'$ , two black horizons (BHs) that particles can only enter, and two white horizons (WHs) that particles can only exit.

The simplest coordinate system that non-singularly covers both the exterior  $I$  and its BH (WH) is the ingoing (outgoing) Eddington-Finkelstein system, in which we replace Schwarzschild time  $t$  by ingoing (outgoing) Eddington-Finkelstein time  $v_+$  ( $v_-$ ), related by  $dv_{\pm} = dt \pm \frac{dr}{f(r)}$ , so that the line element (1) becomes

$$ds^2 = -f(r)dv_{\pm}^2 \pm 2dv_{\pm}dr + r^2d\Omega^2. \quad (3)$$

Following the classic Gibbons-Hawking analysis [13], in order to extract the quantum/thermodynamic properties of this spacetime, and to define quantum field theory on it, it is standard to start in Schwarzschild coordinates (the coordinates that make manifest the full isometry group of the metric) and then “Wick rotate” to the *Euclidean* Schwarzschild metric, by replacing the Schwarzschild coordinates,  $t$  and  $r$ , by the Euclidean time  $\tau$  and Euclidean radius  $\sigma > 0$ , defined by

$$t(\tau) = -i\tau, \quad r(\sigma) = 2m \left[ 1 + \left( \frac{\sigma}{4m} \right)^2 \right]. \quad (4)$$

<sup>1</sup> We also draw the reader’s attention to several other proposals for variations to the usual black hole geometry or topology [6–11].

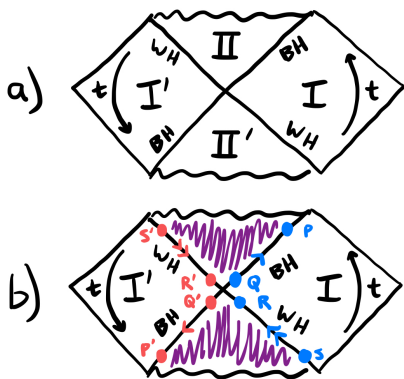


FIG. 1. (a) Penrose diagram for the eternal Schwarzschild (Kruskal) black hole, indicating the two exteriors ( $I, I'$ ), two interiors ( $II, II'$ ), two black horizons (BH), two white horizons (WH), and the time-like killing vector  $\partial_t$ : time flows upward in exterior  $I$ , and downward in exterior  $I'$ . (b) Penrose diagram for eternal Schwarzschild black mirror: exteriors  $I, I'$  are glued together, BH to BH and WH to WH, as indicated (e.g.  $P \sim P', R \sim R'$ ), and with antipodal inversion of the  $(\theta, \varphi)$  2-sphere (see Appendix C), so the interiors  $II, II'$  and their curvature singularities (purple regions) are removed.

So the Euclidean Schwarzschild metric (in  $\tau, \sigma$  coordinates) is given by

$$ds^2 = \frac{2m}{r(\sigma)} \left( \frac{\sigma}{4m} \right)^2 d\tau^2 + \frac{r(\sigma)}{2m} d\sigma^2 + r(\sigma)^2 d\Omega^2. \quad (5)$$

For small  $\sigma$  (which corresponds to the near-horizon limit in Lorentzian signature), this becomes

$$ds^2 \approx \frac{\sigma^2}{(4m)^2} d\tau^2 + d\sigma^2 + (2m)^2 d\Omega^2. \quad (6)$$

One recognizes this as the metric of a 2-dimensional  $(\tau, \sigma)$  cone  $C^2$ , with a 2-dimensional  $(\theta, \varphi)$  sphere  $S^2$  of radius  $2m$  living over each point of the cone (see Fig. 2a). The  $C^2$  has angular coordinate  $\propto \tau$ , and radial coordinate  $\sigma$  measuring the proper distance from the tip  $\sigma = 0$ . Note that, in the standard Euclidean analysis [13], one considers the *one-sided*  $C^2$  (the blue cone in Fig. 2a), corresponding to the black hole exterior region  $I$  ( $\sigma > 0$ ).

Then, if the Euclidean time coordinate's period is precisely  $8\pi m$  (i.e. if we identify  $\tau \sim \tau + 8\pi m$ ), the conic singularity at  $\sigma = 0$  is removed, and the one-sided  $C^2$  (the blue cone in Fig. 2a) becomes a non-singular 2D Euclidean surface (the blue surface in Fig. 2b). From this, one infers that the black hole's temperature  $T_{BH}$  is the inverse of this natural period:  $T_{BH} = 1/8\pi m$  [13].

After this elegant argument, we appear to be left with a smooth, complete Euclidean spacetime (the blue surface in Fig. 2b) which is usually regarded as the entire Euclidean Schwarzschild metric. But this blue surface corresponds purely to the Schwarzschild *exterior*  $\sigma > 0$  (region  $I$  in Fig. 1a). What happened to the spacetime *behind* the event horizon at  $\sigma = 0$ ?

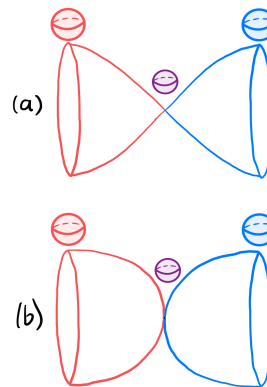


FIG. 2. The Euclidean Schwarzschild metric, with  $\sigma > 0$  in blue, and  $\sigma < 0$  in red. (a) for generic  $\tau$  period: conic singularity; (b) for special  $\tau$  period  $8\pi M$ : no conic singularity.

To answer this question, let us first take a step back to the conical geometry of Fig. 2a. Here it is clear that the single (blue) cone naturally extends to the double (blue+red cone) by letting  $\sigma$  extend to negative values. Then, when we identify  $\tau \sim \tau + 8\pi m$  (removing the conical singularity), we obtain the full (blue+red) Euclidean Schwarzschild metric, Fig. 2b. Note: this full geometry still has nothing corresponding to the black hole *interior*; instead, it has two *exteriors* glued together at  $\sigma = 0$  (an  $S^2$  of area  $16\pi m^2$ , corresponding to the horizon).

Further evidence for the two-sided geometry in Fig. 2b comes from black hole entropy. Gibbons and Hawking [13] compute the entropy of the Schwarzschild black hole by computing the action of the Euclidean Schwarzschild metric (which comes entirely from the Gibbons-Hawking-York boundary term [13, 14]). And, because they compute this action for the *one-sided* (blue) spacetime, they obtain a non-zero answer. This is a clue that the one-sided Euclidean metric is physically incomplete. If, instead, we compute the action/entropy for the two-sided Euclidean spacetime, the answer vanishes (as the two boundary terms, on isometric but oppositely oriented boundaries, make equal and opposite contributions, see Appendix B). This suggests a picture in which the full (blue+red) geometry corresponds to the full (pure, zero entropy) quantum state, while the half (blue) geometry corresponds to the mixed state obtained by tracing out the other (red) half; and the black hole entropy corresponds to the entanglement entropy (i.e. the von Neumann entropy of the blue side, after tracing out the red side). This in turn explains why the entropy is proportional to the area of the horizon (since the entanglement entropy between two regions is characteristically proportional to the size of the boundary separating them).

If we Wick rotate the full Euclidean metric (5) back to Lorentzian signature using  $\tau = it$ , we obtain a metric that now covers the full exterior  $r > 2m$  in Fig. 1a (i.e. regions  $I$  and  $I'$ ). This is the Einstein-Rosen bridge [1], which is incomplete as it stands, and needs to be ex-

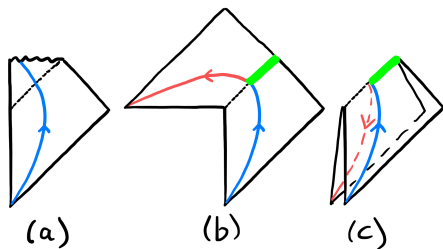


FIG. 3. The Penrose diagram for: (a) a black hole formed by gravitational collapse; or (b,c) a black mirror formed by gravitational collapse, in unfolded view (b) or folded view (c). Some infalling particle trajectories are also shown, with the angular  $S^2$  over each point on the right (blue) side the antipodal inverse of the one on the left, see Appendix C.

tended to a complete spacetime. The conventional completion is the Kruskal extension of Fig. 1a; but here we suggest a different completion. The simplest way to introduce this alternative possibility is to extend the metric to the horizon by replacing  $t$ , as before, with the ingoing (outgoing) Eddington-Finkelstein time coordinate  $v_+$  ( $v_-$ ). Then the metric becomes

$$ds^2 = -\frac{2m}{r(\sigma)} \left(\frac{\sigma}{4m}\right)^2 dv_{\pm}^2 \pm \frac{\sigma}{2m} d\sigma dv_{\pm} + r(\sigma)^2 d\Omega^2. \quad (7)$$

Now notice that, in order for this extension to be well-defined (to not assign the same  $v, \sigma$  coordinate to two distinct points), we are forced (as shown in Fig. 1b) to identify the two BH horizons (e.g.  $P \sim P', Q \sim Q'$ ) and similarly the two WH horizons (e.g.  $R \sim R', S \sim S'$ ).<sup>2</sup> This has the effect of gluing the exterior  $I$  directly to the exterior  $I'$ , which together form a complete spacetime.

The resulting spacetime is the simplest (Schwarzschild) black mirror: eternal, static, uncharged. It is described by the metric (7), with  $-\infty < v < \infty$  and  $-\infty < \sigma < \infty$ . More precisely, the ingoing (outgoing) Eddington-Finkelstein coordinates  $v_+, \sigma$  ( $v_-, \sigma$ ) cover the whole spacetime *except* the WH (BH), and these two coordinate systems together form a complete atlas. We see that, in  $v, \sigma$  coordinates, all components of the metric are explicitly smooth, analytic and finite functions of  $v, \sigma$  (for all  $-\infty < v, \sigma < \infty$ ); and one can check that all associated curvature tensors and invariants (such as the Kretschmann scalar) are as well.

Note that the Lorentzian and Euclidean geometries are now in perfect correspondence: in both, the  $\sigma = 0$  surface (i.e. the origin of the double cone in Euclidean signature, or the event horizon in Lorentzian signature) serves as the boundary between two mirror-image *exterior* regions, with no interior regions or curvature singularities.

<sup>2</sup> Note that we do *not* identify *all* antipodal pairs in Fig. 1a, as has sometimes been considered in the past [6]; in particular, we do not identify points in exterior  $I$  with points in exterior  $I'$ .

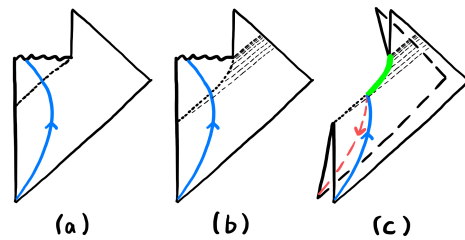


FIG. 4. (a) Traditional Penrose diagram for a black hole which collapses, then evaporates; (b) Improved Penrose diagram indicating shrinking of horizon due to Hawking radiation; (c) Black mirror which collapses, then evaporates.

But there is no free lunch! Although we have gotten rid of all curvature singularities, they have been replaced by another (milder) singularity. In particular, if we compute the eigenvalues of  $g_{\mu\nu}$  (in  $v, \sigma$  coordinates) then, in addition to the angular eigenvalues  $\lambda_{\theta} = r^2(\sigma)$  and  $\lambda_{\varphi} = r^2(\sigma)\sin^2\theta$ , we see the remaining two (positive and negative) eigenvalues

$$\lambda_{\pm} = -\frac{\sigma}{4r(\sigma)} \left( \frac{\sigma}{4m} \pm \sqrt{\frac{r(\sigma)^2}{m^2} + \frac{\sigma^2}{16m^2}} \right) \quad (8)$$

swap places across the horizon,  $\lambda_+(\sigma) = \lambda_-(-\sigma)$ ; so  $\lambda_{\pm}(\sigma)$  both have simple analytic zeros at  $\sigma = 0$  (while the corresponding eigenvalues  $\lambda_{\pm}^{-1}$  of  $g^{\mu\nu}$  have simple poles).

In the standard black hole solution, we are used to the fact that, if some eigenvalues of  $g_{\mu\nu}$  approach zero or infinity as we approach the horizon, this is a mere coordinate singularity that can be removed by an appropriate change of coordinates. But in the black mirror, this is not possible – in coordinates where the metric is smooth and continuous across the horizon, the simple zeros in two eigenvalues of  $g_{\mu\nu}$  are unavoidable: they represent a genuine (but mild) singularity in the geometry, closely related to the singularity joining the two sides of the Euclidean Schwarzschild spacetime in Fig. 2b; and the corresponding simple poles in  $g^{\mu\nu}$  represent real phenomena, akin to the poles we go around in defining the Feynman propagator. We will explain their meaning below.

But first note that, although we have so far focused for simplicity on the Schwarzschild (i.e. 4D non-rotating, non-charged, asymptotically flat) black mirror, all the analysis and discussion extends directly – without any qualitative changes – to the most general 4D *stationary* black mirror (including rotation, electric and magnetic charge, and a non-zero cosmological constant). This is explained in detail in Appendix A. One can similarly obtain the spinning (A)dS black mirror in arbitrary dimensions, starting from the solution in [15, 16].

### III. DISCUSSION

So far, we have considered the general stationary black mirror. Now let us explain how we think the gen-

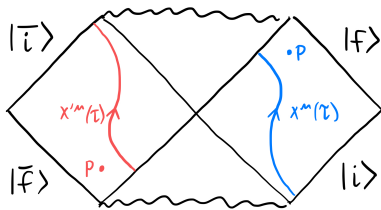


FIG. 5. Asymptotically flat spacetime with CPT-symmetric boundary conditions: states  $|\bar{i}\rangle$  and  $|f\rangle$  are the CPT conjugates of states  $|i\rangle$  and  $|f\rangle$ , respectively (see Appendix C).

eral time-dependent case works. (Since this part of the story can no longer be described explicitly analytically, it is correspondingly less certain and more speculative.) We start with the Penrose diagram in Fig. 3a for an asymptotically-flat black hole formed by realistic gravitational collapse, with a blue curve showing the trajectory of an infalling particle (the arrow shows the direction of flow of electric charge). The corresponding black mirror is again obtained by identifying two CPT mirror copies of the exterior at their respective horizons, as in Fig. 3b: now we see that the (blue) particle falling into the BH from one side meets its CPT mirror (red) anti-particle falling in from the other side. For visualization, it is convenient to fold the diagram in Fig. 3b to obtain the diagram shown in Fig. 3c. In this folded picture, time runs in its usual upward direction on both sheets, and we can explicitly see that both sheets share a common *future* null boundary (*i.e.*, a BH).

In the stationary case, the event horizon and apparent horizon coincide. More generally, where they do not, we conjecture the correct matching surface is the *apparent horizon* (which is well-defined to linear order in perturbations around the stationary solution [17]) since: (i) it is defined locally (unlike the event horizon); and (ii) it appears to be the surface associated to dynamical black hole entropy [17] which, as argued above, is also naturally associated to the surface separating the two exteriors of a black mirror. This suggests the potential, at least in principle, of observationally distinguishing dynamical black mirrors from dynamical black holes, *e.g.* via gravitational wave observations.

Finally, some further hints favoring black mirrors:

i) It is natural to consider the path integral for our universe with CPT-symmetric boundary conditions as shown in Fig. 6 (see Appendices B, C). Whereas the black hole (Fig. 1a) and black mirror (Fig. 1b) both satisfy these boundary condition, the black mirror seems to be the relevant saddle point as it (i) is free of curvature singularities, and (ii) has no *additional* boundaries (whereas the black hole solution has additional boundaries which are singular and also require further data to be specified).

ii) According to an external observer, an infalling object appears to take infinitely long to reach the BH. In the standard account [2], this is an optical illusion: the infalling object actually crosses the horizon into the in-

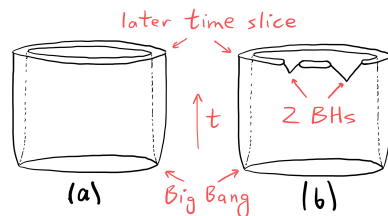


FIG. 6. The Penrose diagram for: (a) an unperturbed CPT-symmetric universe; a CPT-symmetric universe with two black mirrors.

terior, but it takes infinitely long for the visual evidence to reach the exterior observer. However, taking quantum effects into account, the external observer sees the BH evaporate in a *finite* time, *before* the infalling object reaches the horizon, contradicting the standard account and drawing the interior's existence into question [18–20].

iii) The black hole information paradox [4] and firewall paradox [5] come from imagining that quantum information falls into a black hole, and asking how it can re-emerge (particularly since the black hole interior is causally disconnected from future null infinity, see Figs. 3a, 4a). In the black mirror Fig. 3c, with no interior, the puzzle is resolved: when a (blue) particle and (red) anti-particle meet at the horizon, they annihilate into (green) radiation that propagates along the horizon (classically), or gradually leaks off the horizon (quantumly), until the black hole evaporates (Fig. 4b).

iv) As a black hole settles to stationarity, we *expect* it to approach a thermal state, which should also be CPT-symmetric [21]. The black hole (Fig. 3a) does not do this (it settles down to a spacetime with a BH and no WH, with no way for CPT to act), but the black mirror (Fig. 3b, 4b) *does* (see Appendix C). (Hawking also argued that CPT conflicts with black hole interiors [22].)

v) In the standard picture, one can drop global net charge into a black hole, which is then erased when the hole evaporates, leading to the lore that quantum gravity violates global symmetries [23–26]. By contrast, in the black mirror, global charge falling in on one side is canceled by anti-charge falling in on the other; so black mirror evaporation does *not* imply violation of global symmetry. This is compatible with the fact that in the standard model  $B - L$  is anomaly free and might be exact.

vi) This CPT-symmetric picture for black mirrors fits naturally in the CPT-symmetric picture of the cosmos advocated in [27–34] (see Fig. 6): the two sheets of spacetime split at the Bang, and merge at BHs. As before, it is natural to regard the two-sheeted spacetime as representing a pure state, while one sheet represents the mixed state obtained by tracing over the other sheet. This neatly explains why the corresponding entropy, associated with the boundary surface separating the two sheets, is given by the *horizon area* (in the BH case) [13, 35, 36], and the *total comoving spatial volume* (in the cosmological case [32, 33]).



## ACKNOWLEDGMENTS

KT wishes to thank Mihalis Dafermos and Matt Visser for their helpful comments during the Strong Gravity conference. LB is grateful to Minhyong Kim for helpful discussions. KT, LB, and NT are supported by the STFC Consolidated Grant ‘Particle Physics at the Higgs

Centre’, and NT is supported by the Higgs Chair at the University of Edinburgh. Research at Perimeter Institute is supported by the Government of Canada, through Innovation, Science and Economic Development, Canada and by the Province of Ontario through the Ministry of Research, Innovation and Science.

- 
- [1] Albert Einstein and N. Rosen, “The Particle Problem in the General Theory of Relativity,” *Phys. Rev.* **48**, 73–77 (1935).
- [2] J. R. Oppenheimer and H. Snyder, “On continued gravitational contraction,” *Phys. Rev.* **56**, 455–459 (1939).
- [3] Mihalis Dafermos and Jonathan Luk, “The interior of dynamical vacuum black holes I: The  $C^0$ -stability of the Kerr Cauchy horizon,” (2017), [arXiv:1710.01722 \[gr-qc\]](#).
- [4] S. W. Hawking, “Breakdown of Predictability in Gravitational Collapse,” *Phys. Rev. D* **14**, 2460–2473 (1976).
- [5] Ahmed Almheiri, Donald Marolf, Joseph Polchinski, and James Sully, “Black Holes: Complementarity or Firewalls?” *JHEP* **02**, 062 (2013), [arXiv:1207.3123 \[hep-th\]](#).
- [6] G. W. Gibbons, “The elliptic interpretation of black holes and quantum mechanics,” *Nucl. Phys. B* **271**, 497–508 (1986).
- [7] Mehdi Saravani, Niayesh Afshordi, and Robert B. Mann, “Empty black holes, firewalls, and the origin of Bekenstein–Hawking entropy,” *Int. J. Mod. Phys. D* **23**, 1443007 (2015), [arXiv:1212.4176 \[hep-th\]](#).
- [8] Matt Visser, “Traversable wormholes: Some simple examples,” *Phys. Rev. D* **39**, 3182–3184 (1989), [arXiv:0809.0907 \[gr-qc\]](#).
- [9] Matt Visser, “Traversable wormholes from surgically modified Schwarzschild space-times,” *Nucl. Phys. B* **328**, 203–212 (1989), [arXiv:0809.0927 \[gr-qc\]](#).
- [10] Gerard ’t Hooft, “Black hole unitarity and antipodal entanglement,” *Found. Phys.* **46**, 1185–1198 (2016), [arXiv:1601.03447 \[gr-qc\]](#).
- [11] Gerard ’t Hooft, “The Firewall Transformation for Black Holes and Some of Its Implications,” *Found. Phys.* **47**, 1503–1542 (2017), [arXiv:1612.08640 \[gr-qc\]](#).
- [12] Ray d’Inverno, *Introducing Einstein’s relativity* (Oxford University Press, 1992).
- [13] G. W. Gibbons and S. W. Hawking, “Action Integrals and Partition Functions in Quantum Gravity,” *Phys. Rev. D* **15**, 2752–2756 (1977).
- [14] James W. York, Jr., “Role of conformal three geometry in the dynamics of gravitation,” *Phys. Rev. Lett.* **28**, 1082–1085 (1972).
- [15] G. W. Gibbons, H. Lu, Don N. Page, and C. N. Pope, “Rotating black holes in higher dimensions with a cosmological constant,” *Phys. Rev. Lett.* **93**, 171102 (2004), [arXiv:hep-th/0409155](#).
- [16] G. W. Gibbons, H. Lu, Don N. Page, and C. N. Pope, “The General Kerr-de Sitter metrics in all dimensions,” *J. Geom. Phys.* **53**, 49–73 (2005), [arXiv:hep-th/0404008](#).
- [17] Stefan Hollands, Robert M. Wald, and Victor G. Zhang, “Entropy of dynamical black holes,” *Phys. Rev. D* **110**, 024070 (2024), [arXiv:2402.00818 \[hep-th\]](#).
- [18] Tanmay Vachaspati, Dejan Stojkovic, and Lawrence M. Krauss, “Observation of incipient black holes and the information loss problem,” *Phys. Rev. D* **76**, 024005 (2007), [arXiv:gr-qc/0609024](#).
- [19] Tanmay Vachaspati and Dejan Stojkovic, “Quantum radiation from quantum gravitational collapse,” *Phys. Lett. B* **663**, 107–110 (2008), [arXiv:gr-qc/0701096](#).
- [20] Hikaru Kawai, Yoshinori Matsuo, and Yuki Yokokura, “A Self-consistent Model of the Black Hole Evaporation,” *Int. J. Mod. Phys. A* **28**, 1350050 (2013), [arXiv:1302.4733 \[hep-th\]](#).
- [21] Geoffrey L. Sewell, “Quantum fields on manifolds: PCT and gravitationally induced thermal states,” *Annals Phys.* **141**, 201–224 (1982).
- [22] S. W. Hawking, “Information Preservation and Weather Forecasting for Black Holes,” (2014), [arXiv:1401.5761 \[hep-th\]](#).
- [23] S. W. Hawking, “Particle Creation by Black Holes,” *Commun. Math. Phys.* **43**, 199–220 (1975), [Erratum: *Commun. Math. Phys.* **46**, 206 (1976)].
- [24] Edward Witten, “Symmetry and Emergence,” *Nature Phys.* **14**, 116–119 (2018), [arXiv:1710.01791 \[hep-th\]](#).
- [25] Daniel Harlow and Hiroshi Ooguri, “Constraints on Symmetries from Holography,” *Phys. Rev. Lett.* **122**, 191601 (2019), [arXiv:1810.05337 \[hep-th\]](#).
- [26] Daniel Harlow and Hiroshi Ooguri, “Symmetries in quantum field theory and quantum gravity,” *Commun. Math. Phys.* **383**, 1669–1804 (2021), [arXiv:1810.05338 \[hep-th\]](#).
- [27] Latham Boyle, Kieran Finn, and Neil Turok, “CPT-Symmetric Universe,” *Phys. Rev. Lett.* **121**, 251301 (2018), [arXiv:1803.08928 \[hep-ph\]](#).
- [28] Latham Boyle, Kieran Finn, and Neil Turok, “The Big Bang, CPT, and neutrino dark matter,” *Annals Phys.* **438**, 168767 (2022), [arXiv:1803.08930 \[hep-ph\]](#).
- [29] Latham Boyle and Neil Turok, “Two-Sheeted Universe, Analyticity and the Arrow of Time,” (2021), [arXiv:2109.06204 \[hep-th\]](#).
- [30] Latham Boyle and Neil Turok, “Cancelling the vacuum energy and Weyl anomaly in the standard model with dimension-zero scalar fields,” (2021), [arXiv:2110.06258 \[hep-th\]](#).
- [31] Latham Boyle, Martin Teuscher, and Neil Turok, “The Big Bang as a Mirror: a Solution of the Strong CP Problem,” (2022), [arXiv:2208.10396 \[hep-ph\]](#).
- [32] Neil Turok and Latham Boyle, “Gravitational entropy and the flatness, homogeneity and isotropy puzzles,” *Phys. Lett. B* **849**, 138443 (2024), [arXiv:2201.07279 \[hep-th\]](#).
- [33] Latham Boyle and Neil Turok, “Thermodynamic solution of the homogeneity, isotropy and flatness puzzles (and a clue to the cosmological constant),” *Phys. Lett. B* **849**, 138442 (2024), [arXiv:2210.01142 \[gr-qc\]](#).
- [34] Neil Turok and Latham Boyle, “A Minimal Explanation of the Primordial Cosmological Perturbations,” (2023),

arXiv:2302.00344 [hep-ph].

- [35] J. D. Bekenstein, “Black holes and the second law,” *Lett. Nuovo Cim.* **4**, 737–740 (1972).
- [36] Jacob D. Bekenstein, “Black holes and entropy,” *Phys. Rev. D* **7**, 2333–2346 (1973).
- [37] B. Carter, “Hamilton-Jacobi and Schrodinger separable solutions of Einstein’s equations,” *Commun. Math. Phys.* **10**, 280–310 (1968).
- [38] B. Carter, “Black holes equilibrium states,” in *Les Houches Summer School of Theoretical Physics: Black Holes* (1973) pp. 57–214.
- [39] J. F. Plebanski and M. Demianski, “Rotating, charged, and uniformly accelerating mass in general relativity,” *Annals Phys.* **98**, 98–127 (1976).
- [40] Marco M. Caldarelli, Guido Cognola, and Dietmar Klemm, “Thermodynamics of Kerr-Newman-AdS black holes and conformal field theories,” *Class. Quant. Grav.* **17**, 399–420 (2000), arXiv:hep-th/9908022.
- [41] Sidney Coleman, *Aspects of Symmetry: Selected Erice Lectures* (Cambridge University Press, Cambridge, U.K., 1985).
- [42] E. C. G. Stueckelberg, “La signification du temps propre en mécanique ondulatoire,” *Helvetica physica acta* **14**, 322–323 (1941).
- [43] Ernst Carl Gerlach Stueckelberg Stueckelberg, “Un nouveau modele de l’électron ponctuel en théorie classique,” *Helv. Phys. Acta* **14**, 51–80 (1941).
- [44] E. C. G. Stueckelberg, “Remarks on the creation of pairs of particles in the theory of relativity,” *Helv. Phys. Acta* **14**, 588–594 (1941).

## Appendix A: General Stationary Black Mirror

### 1. Boyer-Lindquist coordinates

Consider the general charged, rotating black hole exterior in dS or AdS [37–40]. We start in generalized Boyer-Lindquist coordinates  $(t, r, \theta, \phi)$  – the generalization of the Schwarzschild coordinates considered Section II. We define the tetrad

$$e^0 = \frac{\Delta_r^{1/2}}{\rho} (dt - \frac{a \sin^2 \theta}{\Xi} d\phi) \quad (\text{A1a})$$

$$e^1 = \frac{\rho}{\Delta_r^{1/2}} dr \quad (\text{A1b})$$

$$e^2 = \frac{\rho}{\Delta_\theta^{1/2}} d\theta \quad (\text{A1c})$$

$$e^3 = \frac{\Delta_\theta^{1/2} \sin \theta}{\rho} (a dt - \frac{r^2 + a^2}{\Xi} d\phi) \quad (\text{A1d})$$

where we have defined

$$\begin{aligned} \Delta_\theta &\equiv 1 - \frac{a^2}{\ell^2} \cos^2 \theta, & \Delta_r &\equiv (r^2 + a^2) \left(1 + \frac{r^2}{\ell^2}\right) - 2mr + q^2, \\ \rho^2 &\equiv r^2 + a^2 \cos^2 \theta, & \Xi &\equiv 1 - \frac{a^2}{\ell^2}, \end{aligned} \quad (\text{A2})$$

with  $a$  the rotation parameter,  $\ell$  the AdS radius, and  $q^2 = q_e^2 + q_m^2$ , with  $q_e$  and  $q_m$  the electric and magnetic

charges, respectively. (To obtain the corresponding dS black hole, just make the substitution  $\ell^2 \rightarrow -\ell^2$ .) Then the line element is

$$ds^2 = \eta_{ab} e^a e^b \quad \eta_{ab} = \text{diag}(-1, 1, 1, 1) \quad (\text{A3a})$$

and the electromagnetic potential  $A = A_\mu dx^\mu$  and field strength  $F = dA = F_{\mu\nu} dx^\mu \wedge dx^\nu$  are given by

$$A = -\frac{q_e r}{\Delta_r^{1/2} \rho} e^0 - \frac{q_m \cos \theta}{\Delta_\theta^{1/2} \rho \sin \theta} e^3 \quad (\text{A3b})$$

and

$$\begin{aligned} F &= -\frac{1}{\rho^4} [q_e (r^2 - a^2 \cos^2 \theta) + 2q_m r a \cos \theta] e^0 \wedge e^1 \\ &+ \frac{1}{\rho^4} [q_m (r^2 - a^2 \cos^2 \theta) - 2q_e r a \cos \theta] e^2 \wedge e^3. \end{aligned} \quad (\text{A3c})$$

Note that if  $m < m_{extr}$ , where  $m_{extr}$  is defined in Eq. (8) in Caldarelli, Cognola and Klemm (1999), then the black hole is super-extremal;  $\Delta_r$  has no real roots and hence no horizons, and a naked singularity. We will henceforth assume the opposite, that  $m > m_{extr}$ , so that the black hole is sub-extremal, with two real roots,  $r_-$  and  $r_+$ . The BH horizon is located at the outer root  $r_+$ , and the horizon area is given by

$$\mathcal{A}_{BH} = \frac{4\pi(r_+^2 + a^2)}{\Xi}. \quad (\text{A4})$$

Boyer-Lindquist coordinates make manifest the full symmetry of the exterior spacetime: two Killing vectors  $\partial/\partial t$  and  $\partial/\partial \phi$ , and two discrete symmetries which send  $(t, r, \theta, \phi)$  to, respectively,  $(t, r, \pi - \theta, \phi)$  and  $(-t, r, \theta, -\phi)$ .

### 2. Going Euclidean, thermodynamics

To construct the Euclidean metric, we start with Boyer-Lindquist coordinates  $(t, r, \theta, \phi)$ , and make the Wick rotations  $t = i\tau$ ,  $a = i\hat{a}$ ,  $q = i\hat{q}$ , and consider real values of  $\tau$ ,  $\hat{a}$ , and  $\hat{q}$ , thus obtaining the new tetrad

$$e^0 = \frac{\hat{\Delta}_r^{1/2}}{\hat{\rho}} (d\tau - \frac{\hat{a} \sin^2 \theta}{\hat{\Xi}} d\phi) \quad (\text{A5a})$$

$$e^1 = \frac{\hat{\rho}}{\hat{\Delta}_r^{1/2}} dr \quad (\text{A5b})$$

$$e^2 = \frac{\hat{\rho}}{\hat{\Delta}_\theta^{1/2}} d\theta \quad (\text{A5c})$$

$$e^3 = \frac{\hat{\Delta}_\theta^{1/2} \sin \theta}{\hat{\rho}} (-\hat{a} d\tau - \frac{r^2 - \hat{a}^2}{\hat{\Xi}} d\phi) \quad (\text{A5d})$$

where

$$\begin{aligned} \hat{\Delta}_\theta &\equiv 1 + \frac{\hat{a}^2}{\ell^2} \cos^2 \theta, & \hat{\Delta}_r &\equiv (r^2 - \hat{a}^2) \left(1 + \frac{r^2}{\ell^2}\right) - 2mr - \hat{q}^2, \\ \hat{\rho}^2 &\equiv r^2 - \hat{a}^2 \cos^2 \theta, & \hat{\Xi} &\equiv 1 + \frac{\hat{a}^2}{\ell^2}. \end{aligned} \quad (\text{A6})$$

Then the Euclidean line element is

$$ds^2 = \delta_{ab} \hat{e}^a \hat{e}^b \quad (\text{A7})$$

Next we switch radial coordinate  $r \rightarrow \sigma$ , by making the substitution

$$r(\sigma) \rightarrow \hat{r}_+ + \alpha^2 \sigma^2 \quad \Rightarrow \quad dr \rightarrow 2\alpha^2 \sigma d\sigma \quad (\text{A8})$$

where  $\hat{r}_+$  is the Wick rotation of the previous horizon radius  $r_+$  (and a root of  $\hat{\Delta}_r$ ), the constant  $\alpha$  is determined below. Then, to leading order in  $\sigma$ , the metric becomes

$$ds^2 = \frac{4\alpha^2 \hat{\rho}_+^2}{\hat{\Delta}'_r(\hat{r}_+)} (d\sigma^2 + \sigma^2 d\hat{\omega}_1^2) + \frac{\hat{\rho}_+^2}{\hat{\Delta}_\theta} (d\theta^2 + \sin^2 \theta d\hat{\omega}_2^2) \quad (\text{A9})$$

where

$$d\hat{\omega}_1 = \frac{\hat{\Delta}'_r(\hat{r}_+)}{2\hat{\rho}_+^2} (d\tau - \frac{\hat{a} \sin^2 \theta}{\hat{\Xi}} d\phi) \quad (\text{A10a})$$

$$d\hat{\omega}_2 = \frac{\hat{\Delta}_\theta}{\hat{\rho}_+^2} (\hat{a} d\tau + \frac{r_+^2 - \hat{a}^2}{\hat{\Xi}} d\phi) \quad (\text{A10b})$$

and we see that, by choosing  $\alpha^2 = \hat{\Delta}'_r(\hat{r}_+) / (4\hat{\rho}_+^2)$  we can set the leading coefficient in (A9) to unity.

As in the Schwarzschild case, we see the Euclidean metric has the topology  $C^2 \times S^2$  of a one-sided 2-cone  $C^2$  (parameterized by  $\tau, \sigma$ , with its tip at  $\sigma = 0$ ) times a 2-sphere  $S^2$  (parameterized by  $\theta, \varphi$ ) – *i.e.* the blue side of Fig. 2a. And, as before, we can analytically extend this to a 2-sided cone by letting  $\sigma$  extend to negative values (the blue+red surface in Fig. 2a). Note that this extended metric now has a new  $\mathbb{Z}_2$  isometry  $\sigma \rightarrow -\sigma$ .

In order to make the metric smooth at the cone's tip (to remove the conic singularity, as in Fig. 2b), we must identify  $\hat{\omega}_1 \sim \hat{\omega}_1 + 2\pi$ ; and, in since this identification must be  $\theta$ -independent, we are forced to identify

$$(\tau, \phi) \sim (\tau + 2\pi\hat{\beta}, \varphi + 2\pi i\hat{\Omega}\hat{\beta}) \quad (\text{A11})$$

where

$$\hat{\beta} = \frac{2(\hat{r}_+^2 - \hat{a}^2)}{\hat{\Delta}'_r(\hat{r}_+)} \quad (\text{A12a})$$

$$\hat{\Omega} = \frac{i\hat{a}\hat{\Xi}}{\hat{r}_+^2 - \hat{a}^2}. \quad (\text{A12b})$$

Note that this same shift leaves  $\omega_2$  invariant.

Now, Wick-rotating back to Lorentzian signature, and expressing everything in terms of our original Lorentzian variables, we have the identification

$$(t, \phi) \sim (t + 2\pi i\beta, \varphi + 2\pi i\Omega\beta) \quad (\text{A13})$$

where

$$\beta = \frac{2(r_+^2 + a^2)}{\Delta'_r(r_+)}, \quad (\text{A14a})$$

$$\Omega = \frac{a\Xi}{r_+^2 + a^2}. \quad (\text{A14b})$$

Here  $\beta$  is identified as the temperature of the black hole, and  $\Omega$  as the angular velocity of the horizon.

### 3. In Eddington-Finkelstein coordinates

Although the Boyer-Lindquist system has the advantage that it makes manifest the full symmetry of the metric, it has the disadvantage that it only covers the exterior  $r > r_+$ , and fails to extend to (or beyond) the black and white horizons (where it becomes singular). To fix this, we first define new generalized ingoing/outgoing Eddington-Finkelstein coordinates  $(v_\pm, r, \theta, \hat{\phi})$  that remain non-singular on one horizon or the other, by a coordinate transformation of the form

$$dv = dt + \alpha_t dr \quad (\text{A15a})$$

$$d\hat{\phi} = d\phi + \alpha_\phi dr \quad (\text{A15b})$$

where  $\alpha_t = \alpha_t(r)$  and  $\alpha_\phi = \alpha_\phi(r)$  are chosen to make the  $dr^2$  term drop out of the line element  $ds^2$  in the new (Eddington-Finkelstein) coordinate system. One can check that this implies

$$\alpha_t \equiv \pm \frac{r^2 + a^2}{\Delta_r} \quad (\text{A16a})$$

$$\alpha_\phi \equiv \pm \frac{a\Xi}{\Delta_r} \quad (\text{A16b})$$

where the  $+/-$  sign corresponds to ingoing/outgoing Eddington-Finkelstein coordinates which cover the exterior and black/white horizon, respectively.

In these new coordinates, if we define the new tetrad

$$\hat{e}^0 = dv - \frac{a \sin^2 \theta}{\Xi} d\hat{\phi} \quad (\text{A17a})$$

$$\hat{e}^1 = dr \quad (\text{A17b})$$

$$\hat{e}^2 = \frac{\rho}{\Delta_\theta^{1/2}} d\theta \quad (\text{A17c})$$

$$\hat{e}^3 = \frac{\Delta_\theta^{1/2} \sin \theta}{\rho} (a dv - \frac{r^2 + a^2}{\Xi} d\hat{\phi}) \quad (\text{A17d})$$

the line element is

$$ds^2 = \tilde{\eta}_{ab} \hat{e}^a \hat{e}^b, \quad \tilde{\eta}_{ab} = \begin{pmatrix} -\frac{\Delta_r}{\rho^2} & \pm 1 & 0 & 0 \\ \pm 1 & 0 & 0 & 0 \\ 0 & 0 & 1 & 0 \\ 0 & 0 & 0 & 1 \end{pmatrix} \quad (\text{A18a})$$

the gauge potential is

$$A = -\frac{q_e r}{\rho^2} \hat{e}^0 - \frac{q_m \cos \theta}{\Delta_\theta^{1/2} \rho \sin \theta} \hat{e}^3 \quad (\text{A18b})$$

(where we removed an additional term  $\pm \frac{q_e r}{\Delta_r} dr$  via a gauge transformation), and the field strength is

$$F = -\frac{1}{\rho^4} [q_e (r^2 - a^2 \cos^2 \theta) + 2q_m r a \cos \theta] \hat{e}^0 \wedge \hat{e}^1 + \frac{1}{\rho^4} [q_m (r^2 - a^2 \cos^2 \theta) - 2q_e r a \cos \theta] \hat{e}^2 \wedge \hat{e}^3. \quad (\text{A18c})$$

We see that these coordinates remain non-singular at the black/white horizon  $r = r_+$  (where  $\Delta_r$  vanishes): the components of  $g_{\mu\nu}$ ,  $A_\mu$  and  $F_{\mu\nu}$  all remain finite, and the metric determinant remains finite and non-zero.

Now, as before, we can switch from  $r \rightarrow \sigma$  by making the substitution (A8) in Eqs. (A17, A18, A18b, A18c) and extending  $\sigma$  to negative values. If we now let the coordinates  $v_+$  and  $\sigma$  (respectively,  $v_-$  and  $\sigma$ ) extend from  $-\infty$  to  $+\infty$ , we obtain the general stationary black mirror, described in ingoing coordinates  $(v_+, \sigma, \theta, \hat{\varphi})$  (respectively, outgoing coordinates  $(v_-, \sigma, \theta, \hat{\varphi})$ ) which cover the entire spacetime except for the black horizon (respectively, white horizon). Taken together, these ingoing and outgoing coordinate systems provide an atlas covering the complete stationary black mirror spacetime.

As before, the extended spacetime now has a new isometry  $\sigma \rightarrow -\sigma$  that takes us back and forth between the two exterior regions ( $I$  and  $I'$ ), which are identified at the horizon, as in Fig. 1b.

Note that, in these  $(v_\pm, \sigma, \theta, \hat{\varphi})$  coordinates, the components of the resulting metric  $g_{\mu\nu}$  and field strength  $F_{\mu\nu}$ , as well as the components of all curvature invariants (such as the Kretschmann scalar  $R_{\alpha\beta\gamma\delta}R^{\alpha\beta\gamma\delta}$ ) are again everywhere explicitly smooth, analytic and finite, so the spacetime has no curvature singularities. But, as in the Schwarzschild case, two of the eigenvalues  $\lambda_\pm$  of the metric  $g_{\mu\nu}$  are exchanged as we cross the horizon,  $\lambda_+(\sigma) = -\lambda_-(-\sigma)$ , and both of these eigenvalues have simple analytic zeros at  $\sigma = 0$ , while the corresponding eigenvalues  $\lambda_\pm^{-1}$  of  $g^{\mu\nu}$  have simple poles).

## Appendix B: Saddle points of the action

In this appendix, we show that the Schwarzschild black mirror presented in Section II is a regular saddle of the Einstein-Hilbert action

$$S = \int_{\mathcal{M}} dV \frac{R}{16\pi} + \text{boundary terms.} \quad (\text{B1})$$

The boundary terms are needed to ensure that the variation of the action yields the Einstein equations when the metric is held fixed on the boundary, with no constraint on its normal derivative there. The Einstein-Hilbert action does not have this property because it involves second derivatives of the metric. However, it can be reduced to an action involving only first derivatives by performing integrations by parts and discarding the boundary terms. The corrected action is then the appropriate one for a quantum path integral between an initial and a final three-geometry.

A general principle, discussed by Coleman [41], states that if an action respects a symmetry  $G$  then saddles of the action restricted to configurations which respect  $G$  are also saddles of the full action. Hence, saddles of the gravitational action restricted to spherically symmetric spacetimes are also saddles of the full gravitational action. Consider the most general spherically symmetric

line element,

$$ds^2 = -a(t, x)^2 dt^2 + 2S(t, x) dt dx + L(t, x)^2 dx^2 + r(x)^2 d\Omega^2. \quad (\text{B2})$$

Here,  $t$  and  $x$  are  $O(3)$ -invariant coordinates. We do not assume the metric is static and include an arbitrary “shift”  $S(t, x)$  as well as a “lapse” function  $L(t, x)$ . One can use the residual coordinate freedom to set  $S(t, x)$  equal to zero and to choose  $r$  as the radial coordinate. However,  $r$  is not a good coordinate for our analytically extended spacetime and it is better to regard it as a function of a coordinate  $x$  which is.

In order to recover the full set of Einstein equations governing such metrics, one must vary the gravitational action before further restricting the coordinates. As we shall see, varying the action with respect to the shift  $S$  yields a constraint that the lapse  $L$  depends only on  $x$ . (This is the crux of Birkhoff’s theorem, that every spherically symmetric solution of the Einstein equations is static.) Similarly, varying the action with respect to  $L$  yields a constraint on  $a$  and  $r$  and their first  $x$  derivatives. After obtaining these constraints, we can redefine the time coordinate to eliminate  $S$  and reparameterize  $x$  to set  $L$  to unity. Finally, by varying the action with respect to  $a$  and  $r$  we obtain the second order field equations. These imply that  $a(t, x)$  has a trivial time dependence which can be removed by reparameterizing  $t$ .

To calculate the action (B1) restricted to spherical symmetric spacetimes, we insert the ansatz (B2) into the Einstein-Hilbert term and integrate by parts to eliminate second derivatives. We need only retain terms of first order in  $S(t, x)$  since it is set to zero after calculating the first order variations. After several integrations by parts, the action reduces (up to terms of higher order in  $S$ ) to

$$S = \frac{1}{2} \int dt dx \left( aL + \frac{r'(ar' + 2ra')}{L} + 2S \frac{rr'\dot{L}}{aL^2} \right), \quad (\text{B3})$$

where dot denotes  $\partial_t$  and prime  $\partial_x$ . Note a crucial subtlety: that in deriving this expression, we have used the *positive* square root of  $\sqrt{-g}$  in the volume form, and we have also taken the orientation on the  $(\theta, \varphi)$  2-sphere to *reverse* as we pass from  $x > 0$  to  $x < 0$ : see Appendix C. Setting the variation with respect to  $S$  zero yields the constraint that  $\dot{L} = 0$ . (As will be seen later, in the solution  $r'/a$  is finite and non-vanishing everywhere.) Varying the action with respect to  $L$  and then setting it to unity yields the constraint

$$2rr'a' = a(1 - r'^2). \quad (\text{B4})$$

Varying the action with respect to  $a$  and  $r$  then yields the two second order field equations

$$r'' = (1 - r'^2)/(2r), \quad (\text{B5a})$$

$$a'' = -(ar')'/r. \quad (\text{B5b})$$

Eq. (B5a) is solved by noticing that  $r(r'^2 - 1)$  is constant, so that  $r'^2 = 1 - 2m/r$  with  $m$  a constant. This



implies  $r'' = m/r^2$ . Now (B4) yields  $a'/a = r''/r'$  which is integrated to obtain  $a = A(t)r'$  with  $A(t)$  an arbitrary function. Assuming it is nonzero, it can be set to unity by redefining the time coordinate via  $\tilde{t} = \int^t dt A(t)$ .

We now impose CPT symmetric boundary conditions. As we shall explain momentarily, CPT will imply that  $a(x)$  is an odd function of  $x$ . To find the solutions explicitly, we set

$$x = m(2\chi + \sinh(2\chi)). \quad (\text{B6})$$

The solution is then  $r = 2m \cosh^2 \chi$ ,  $a = \tanh \chi$  so that, in the  $(t, \chi)$  coordinate system, the line element is

$$ds^2 = -(\tanh \chi)^2 dt^2 + (\cosh \chi)^4 ((4m)^2 d\chi^2 + (2m)^2 d\Omega^2), \quad (\text{B7})$$

with  $-\infty < t, \chi < \infty$ . The time-like one-form  $e^0$  of the tetrad is odd in  $\chi$  and has a simple zero at  $\chi = 0$ , whereas the space-like one-forms  $e^i$  are even and nonzero throughout. The spatial metric is conformal to a cylinder  $\mathbb{R} \times S^2$ , of radius  $2m$ . In the near-horizon limit ( $|\chi| \ll 1$ ) the coordinate  $\chi \approx \sigma/(4m)$  where  $\sigma$  is the proper radial coordinate used in Eqs. (4-7); whereas far from the horizon ( $\chi \rightarrow \pm\infty$ ) the line element (B7) becomes  $\approx -dt^2 + m^2 e^{\pm 4\chi} (d\chi^2 + \frac{1}{4} d\Omega^2)$  which, with  $r = \frac{m}{2} e^{\pm 2\chi}$ , is just Minkowski spacetime.

Note that, the total action (B3) – which is the sum of the Einstein-Hilbert bulk action and the Gibbons-Hawking-York boundary terms – vanishes when we integrate  $dx$  over a symmetric range from  $-X$  to  $+X$ , because the integrand is an odd function of  $x$ .

The method used here can be straightforwardly generalized to spherically symmetric electro-vacuum solutions that are asymptotically flat, de Sitter or anti-de Sitter. This time, after using various equations of motion obtained from the action, the line element takes the form

$$ds^2 = -a^2(x) dt^2 + dx^2 + r^2(x) d\Omega^2 \quad (\text{B8})$$

with

$$r'^2 = 1 - \frac{2m}{r} + \frac{e^2}{r^2} - \Lambda r^2, \quad (\text{B9a})$$

$$a = r'. \quad (\text{B9b})$$

The function  $a = a(r)$  has at most four roots:  $r_-$  which corresponds to the Cauchy horizon,  $r_+$  which corresponds to the event horizon and  $r_c$  which corresponds to the cosmological horizon, with  $r_c = +\infty$  if  $\Lambda \leq 0$ . Since  $a^2 \geq 0$  it follows that the range of  $r$  lies in the interval

$[r_+, r_c]$ . Moreover, CPT symmetry implies that  $r$  obeys  $r'(0) = 0$ , and therefore  $r(0)$  is a root of  $a = a(r)$ . If  $r(0) = r_c$  then the function  $r = r(x)$  is a constant. Thus, the only physical initial conditions for  $r$  are  $r(0) = r_+$  and  $r'(0) = 0$ . Extending this solution to the horizon by changing coordinates from Schwarzschild time  $t$  to Eddington-Finkelstein time  $v$  ( $v_+$  or  $v_-$ ) once again brings us back to the black mirror geometry discussed in the main text.

### Appendix C: CPT symmetry

In the body of the paper, we focused for simplicity on the Schwarzschild (static, uncharged) black mirror, but let us now consider the general stationary black mirror  $\mathcal{M}$  (including charge), to understand the action of CPT symmetry more clearly. For simplicity, assume the mirror has electric charge  $q_e$  but no magnetic charge.

The natural CPT transformation [21] maps a point with coordinates  $(t, x, \theta, \varphi) \rightarrow (t, -x, \pi - \theta, \varphi + \pi)$  or, equivalently,  $(t, \sigma, \theta, \varphi) \rightarrow (t, -\sigma, \pi - \theta, \varphi + \pi)$ . This is an isometry that leaves both the line element  $ds^2 = g_{\mu\nu} dx^\mu dx^\nu$ , as well as the field strength  $F = F_{\alpha\beta} dx^\alpha \wedge dx^\beta$  invariant. However, due to the inversion of the orientation of the two-sphere, the net charge calculated via Gauss's law from the net flux through this two sphere changes sign under this transformation. In this sense, it not only inverts spacetime, but also reverses electric charges, and is thus a CPT transformation.

This isometry maps *e.g.* a point  $P$  with angular coordinate  $(\theta, \varphi)$  near the upper corner of exterior  $I$  to a mirror point  $P'$  near with angular coordinate  $(\pi - \theta, \varphi + \pi)$  near the lower corner of exterior  $I'$  (see Fig. 5).

The trajectory  $x^\mu(\tau)$  of particle of charge  $q$  in the black mirror spacetime, satisfies the equation of motion

$$\ddot{x}^\mu + \Gamma_{\alpha\beta}^\mu \dot{x}^\alpha \dot{x}^\beta = q F^\mu{}_\nu \dot{x}^\nu \quad (\text{C1})$$

where a dot denotes a proper time derivative  $d/d\tau$ . Performing a CPT transformation on the background also maps the trajectory  $x^\mu(\tau)$  to a new trajectory  $x'^\mu(\tau)$ , see Fig. 5. Moreover, since this map reverses the orientation on the  $(\theta, \varphi)$  2-spheres, it not only reverses the charge of the black hole (as measured by Gauss's law using a sphere surrounding the hole), it also reverses the charge of the point particle (again as measured by Gauss's law using a sphere surrounding the point charge). This is why, in Figs. 3, 4, and 5, the arrows showing charge flow (more correctly, the direction of  $q\dot{x}^\mu$ ) in the left-hand (red) trajectories are reversed relative to the corresponding arrows on the right-hand (blue) trajectories.<sup>3</sup>

<sup>3</sup> This insight, that an antiparticle is just a particle moving backward in time – *i.e.* a particle whose “worldline time” (proper

time) has been reversed relative to the “embedding time” (the time direction in the target space) is due to Stueckelberg [42–44].